J Membrane Biol (2009) 227:87–94
DOI 10.1007/s00232-008-9148-y

Effects of Copper on T-Type Ca^{2+} Channels in Mouse Spermatogenic Cells

Liang Lu · Changsong Wang · Xiaohua Gao · Peng Xu · Jun Wang · Qiang Wang · Jie Cheng · Hang Xiao

Received: 16 October 2008 / Accepted: 4 December 2008 / Published online: 7 January 2009

Abstract Low voltage-activated, rapidly inactivating T-type Ca^{2+} channels are found in a variety of cells, where they regulate electrical activity and Ca^{2+} entry. In whole-cell patch-clamp recordings from mouse spermatogenic cells, trace element copper (Cu^{2+}) inhibited T-type Ca^{2+} current ($I_{T\text{-}Ca}$) with IC_{50} of 12.06 μM. Inhibition of $I_{T\text{-}Ca}$ by Cu^{2+} was concentration-dependent and mildly voltage-dependent. When voltage stepped to −20 m*V*, Cu^{2+} (10 μM) inhibited $I_{T\text{-}Ca}$ by 49.6 ± 4.1%. Inhibition of $I_{T\text{-}Ca}$ by Cu^{2+} was accompanied by a shift of −2.23 m*V* in the voltage dependence of steady-state inactivation. Cu^{2+} upshifted the current–voltage (*I-V*) curve. To know the change of the gating kinetics of T-type Ca^{2+} channels, we analyzed the effect of Cu^{2+} on activation, inactivation, deactivation and reactivation of T-type Ca^{2+} channels. Since T-type Ca^{2+} channels are a key component in capacitation and the acrosome reaction, our data suggest that Cu^{2+} can affect male reproductive function through T-type Ca^{2+} channels as a preconception contraceptive material.

L. Lu · X. Gao · P. Xu · J. Wang · Q. Wang · J. Cheng · H. Xiao (✉)
Department of Toxicology, Nanjing Medical University, Nangjing, Jiangsu 210029, People's Republic of China
e-mail: hxiao@njmu.edu.cn

L. Lu
National Shanghai Center for New Drug Safety Evaluation and Research, Institute of Pharmaceutical Industry, Shanghai 201203, People's Republic of China

C. Wang
Wuxi Xihui Center of Disease Control and Prevention of Jiangsu Province, Wuxi, Jiangsu 214000, People's Republic of China

Keywords Copper · T-type Ca^{2+} channel · Patch clamp · Spermatogenic cell · Acrosome reaction

Introduction

Essential trace minerals (ETMs) are minerals that are required for normal growth and development of animals; however, ETMs are normally present in minute quantities in the animal's body and are required in low concentrations in the diet. Although the nutritional requirements for these elements are small, these nutrients can greatly affect reproduction (Hostetler et al. 2003). The necessity of ETMs for support of life is largely unquestioned; however, their requirement for reproduction has not been as extensively studied.

Copper was first shown to be an ETM by Hart (1928). Copper plays an important role in male and female reproduction (Wong et al. 2001; Thomas and Moss 1951; Ebesh et al. 1999). The toxic effect of copper on spermatozoa, which was demonstrated in 1950 by Quatrefages, has often been confirmed. Copper reduces the oxidative processes and glucose consumption, which reduces or abolishes the mobility of sperm. This property is exploited in intrauterine devices. Toxic effects of copper on seminal plasma were manifested in the decrease of motile spermatozoa percentage and increase of malformed sperm cells (Jurasovic and Telisman 1993). Roblero et al. (1996) demonstrated in vitro that copper in intrauterine devices prevented conception. Results showed that copper, at concentrations similar to those released from intrauterine devices, affected the fertilizing capacity of human gametes in vitro and interfered with the sperm–oocyte interaction leading to fertilization.

Intracellular Ca^{2+} regulates many fundamental physiological processes in excitable and nonexcitable cells.

Certainly, this is the case of sperm where the local concentration of intracellular Ca^{2+} ($[Ca^{2+}]_i$) is significantly influenced by Ca^{2+}-permeable channels present in the cell plasma membrane. Among these channels, the voltage-dependent Ca^{2+} channels (Ca_V) of the T-type (Ca_V3) appear to have an eminent role in the acrosome reaction (AR) of some sperm species, though they may participate in other important functions like motility and capacitation (Darszon et al. 2006). Until recently, it had been quite difficult to electrophysiologically study sperm ion channels. The trouble for patch clamping these specialized cells is their small size, complex morphology and plasma membrane rigidity (Darszon et al. 2005). T-type Ca^{2+} channels are expressed during the meiotic and postmeiotic stages of spermatogenesis and are retained in mature sperm. Therefore, the spermatogenic cell, a developmental precursor of mature sperm, is usually used as a model system to study the effects of agents on the channel events in mature sperm (Lievano et al. 1996; Arnoult et al. 1996, 1998; Espinosa et al. 1999, 2000).

In the present study, we investigated the effects of copper on T-type Ca^{2+} channels in mouse spermatogenic cells and demonstrate its role in reproductive functions such as AR and fertilization.

Materials and Methods

Cell Preparation

Spermatogenic cells were obtained as described previously (Santi et al. 1996). Briefly, testes from adult CD1 mice were excised and suspended in ice-cold dissociation solution, containing (in mM) 2 $CaCl_2$, 150 NaCl, 5 KCl, 1 $MgCl_2$, 12 $NaHCO_3$, 1 NaH_2PO_4 and 11 glucose (pH adjusted with NaOH to 7.4). The tunica albuginea was removed and the seminiferous tubules were teased to release cells. The suspension was transferred to a 35-mm plastic recording chamber with the external solution for T-type Ca^{2+} current recording, containing (in mM) 130 NaCl, 10 $CaCl_2$, 3 KCl, 2 $MgCl_2$, 1 $NaHCO_3$, 0.5 NaH_2PO_4, 5 HEPES and 10 glucose (pH adjusted to 7.4 with NaOH). Spermatogenic cells or symplasts at two different stages of differentiation (pachytene spermatocytes and round spermatids) were preferentially observed and used in electrophysiological recordings. Inasmuch as similar results were obtained from both stages, data were pooled for presentation.

Patch-Clamp Recordings

T-type Ca^{2+} currents were recorded using the whole-cell patch-clamp technique (Bai and Shi 2002) at room temperature using a PC2C patch-clamp amplifier (Huazhongkejidaxue, HuBei, China). Borosilicate glass electrodes were pulled using a vertical puller (Narishige Scientific Instrument Laboratoty, Tokyo, Japan; model PP-83) and had a resistance of 2–5 MΩ when filled with the electrode internal solution. The pipette solution contained (in mM) 120 CsCl, 10 CsF, 10 EGTA, 5 HEPES, 4 Mg-ATP and 10 phosphocreatine (pH adjusted to 7.4 with CsOH). Pipette transients were manually compensated before rupturing the patch. After gigaseal and membrane rupture, series resistance was compensated ≥50%. Cell capacitance was measured by integrating the area of the capacitive transient. Linear leak and residual capacity currents were subtracted online using a P/4 standard protocol. Currents were filtered at 1 kHz and digitized at a sampling rate of 10 kHz. Pulse protocol, data capture and analysis of recordings were performed with PClamp (WaveMetrics, Lake Oswego, OR) and Sigmaplot (SPSS, Inc., Chicago, IL) software. Currents of $I_{T\text{-}Ca}$ were elicited by a 200-ms depolarizing step pulse from the holding potential of −90 to −20 m*V*. Pulses from −80 to + 40 m*V* in 10-m*V* increments were used to elicit the membrane currents for obtaining the *I–V* curve. To measure Ca^{2+} channel inactivation at steady state, cells were held for 210 ms at potentials ranging successively from −100 through −45 m*V* prior to a 90-ms step depolarization to a test potential of −20 m*V*.

Drug Application

$CuCl_2$ and $NiCl_2$ (Sigma, St. Louis, MO) was prepared as a 100-mM stock solution in ddH_2O and diluted in the bath solution for each experiment to give the desired final concentration just before use. Bay K8644 (Sigma) was dissolved in dimethylsulfoxide at 10 mM. The aliquot was then diluted to the final concentrations in the recording solution before use.

Data Analysis

The steady-state activation curve was fitted by the Boltzmann equation: $I_{Ca} = g_{Ca\ max}\ (V_m - E_m)/\{1 + \exp[-(V_m - V_{\alpha 1/2})/\kappa_\alpha]\}$, where I_{Ca} is the peak Ca^{2+} current, g_{Ca} max the maximal conductance, V_m the test potential, E_m the reversal potential, $V_{\alpha 1/2}$ the voltage for half-maximal current activation and κ_α the slope factor. Steady-state inactivation curves were fitted with the Boltzmann equation: $I_{Ca}/I_{Ca\ max} = \{1 + \exp[(V - V_{i1/2})/\kappa_i]\}$, where I_{Ca} max is the maximum of peak Ca^{2+} current, *V* the prepulse potential and $V_{i1/2}$ and κ_i the voltage for half-maximal current inactivation and the slope factor, respectively.

Data were expressed as means ± standard error (SEM). Statistical significance was evaluated by means of the two-

tailed Student's *t*-test for paired data. The threshold of significance was $P < 0.05$. The statistical software used was SPSS 11.5 (SPSS, Inc., Chicago, IL).

Results

T-Type Ca^{2+} Channel Current Recording

A family of inward currents obtained from a spermatogenic cell is shown in Fig. 1a. These inward currents were transient, with activation and inactivation kinetics becoming faster at stronger depolarization. The current was not affected by 1 μM Bay K8644, a specific L-type Ca^{2+} channel activator ($n = 4$, Fig. 1b). After addition to 200 μM Ni^{2+}-containing solution, the current was drastically inhibited, 73.31 ± 3.60% ($n = 4$, Fig. 1c). Figure 1d illustrates an *I–V* relationship obtained by averaging data from seven individual cells. The threshold for inward current activation was at about −60 m*V*, and the peak amplitude occurred at about −20 m*V*. These showed properties typical of the T-type Ca^{2+} current. This is in accordance with previous reports that there are only T-type Ca^{2+} channels in spermatogenic cells.

Concentration-Dependent Effects of Cu^{2+} on $I_{T\text{-}Ca}$

Cu^{2+} showed marked effects on T-type Ca^{2+} currents recorded on mouse spermatogenic cells. Cu^{2+} at 0.3, 1, 3, 10 and 30 μM markedly inhibited $I_{T\text{-}Ca}$ by 9.32 ± 0.74% ($n = 8$, $P < 0.05$), 18.40 ± 1.03% ($n = 7$, $P < 0.05$), 33.60 ± 1.73% ($n = 7$, $P < 0.05$), 49.59 ± 4.13% ($n = 5$, $P < 0.05$) and 59.96 ± 3.60% ($n = 8$, $P < 0.05$), respectively (Fig. 2a). With 10 μM Cu^{2+} application, the peak current was decreased to 50.41% (Fig. 2b). In contrast, without Cu^{2+}, the amplitude of $I_{T\text{-}Ca}$ did not change significantly even for 40 min (Fig. 2c). After washout, the peak of $I_{T\text{-}Ca}$ partially returned (Fig. 2b). The effects of Cu^{2+} on the Ca^{2+} currents could not be attributed to the rundown of Ca^{2+} currents.

Effects of Cu^{2+} on *I–V* Relationship of $I_{T\text{-}Ca}$

Cu^{2+} significantly upshifted the *I–V* curve (Fig. 3a). The current density at −20 m*V* declined from 8.38 ± 0.90 to 4.29 ± 0.35 pA/pF ($n = 5$, $P < 0.05$) in the presence of Cu^{2+} at 10 μM. This inhibition was voltage-independent. After Cu^{2+} treatment, the inhibitions were steady from −30 to +30 m*V* (Fig. 3b).

Voltage Dependence of Activation and Steady-State Inactivation

Figure 4 illustrates the activation and inactivation curves for T-type Ca^{2+} channel. Figure 4a, b shows a family of current records obtained with the activation, inactivation protocol, respectively. Figure 4c shows that the activation curve was shifted in the hyperpolarizing direction after 10 μM Cu^{2+} treatment. In control, the half-activation potential ($V_{\alpha½}$) and the slope factor (κ_α) were estimated to be −48.23 ± 1.29 and 7.93 ± 0.99 m*V*, respectively. After exposure to 10 μM Cu^{2+}, $V_{\alpha½}$ and κ_α were shifted to −50.18 ± 1.30 and 8.03 ± 1.03 m*V* ($n = 4$, $P > 0.05$), respectively. The steady-state inactivation curve was also shifted in the hyperpolarizing direction after 10 μM Cu^{2+} treatment (Fig. 4d). The $V_{i½}$ of the inactivation curve and κ_i value changed from −58.33 ± 0.83 and 5.0 ± 0.62 m*V* to −60.56 ± 0.83 and 4.53 ± 0.61 m*V* ($n = 6$, $P < 0.05$), respectively.

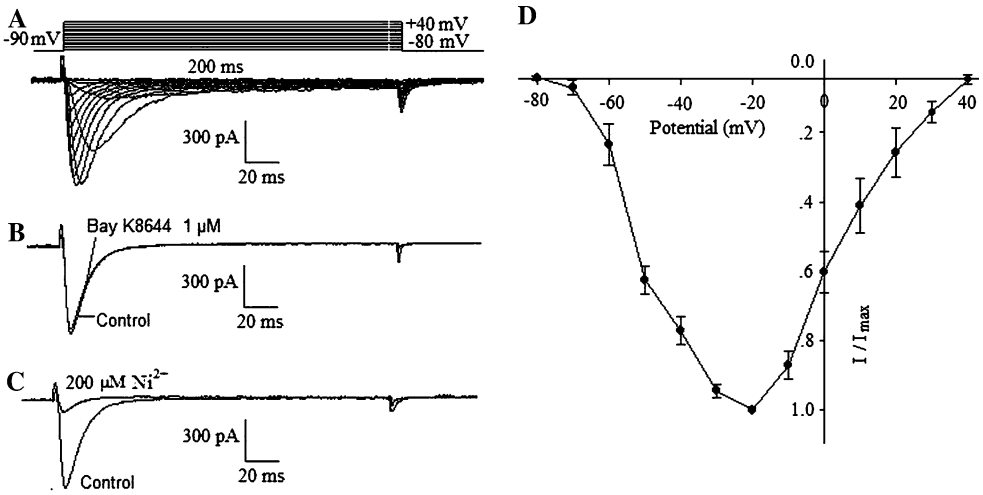

Fig. 1 Whole-cell T-type Ca^{2+} currents in mouse spermatogenic cells. **a** Original records of the currents evoked by a series of depolarizing pulses shown on *top*. **b** Lack of effects of Bay K8644 (1 μM) on the current. **c** Inhibitory effect of 200 μM Ni^{2+} on the current. **d** Mean *I–V* relationship obtained by averaging results from seven individual cells and synplasts. Error bars represent SE

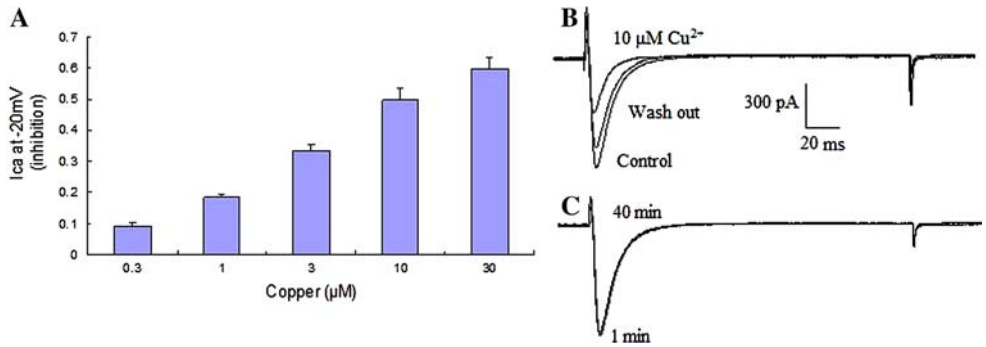

Fig. 2 Effect of Cu^{2+} on T-type Ca^{2+} current in mouse spermatogenic cells. **a** Cu^{2+} inhibited T-type Ca^{2+} current in different concentration conditions. **b** Change of T-type Ca^{2+} current after 10 μM Cu^{2+} treatment and washout. **c** Stability of T-type Ca^{2+} current during the recording period of 40 min without Cu^{2+}. T-type Ca^{2+} current was induced by 200-ms depolarization from a hold potential (HP) of –90 m*V* to a test potential of −20 m*V*

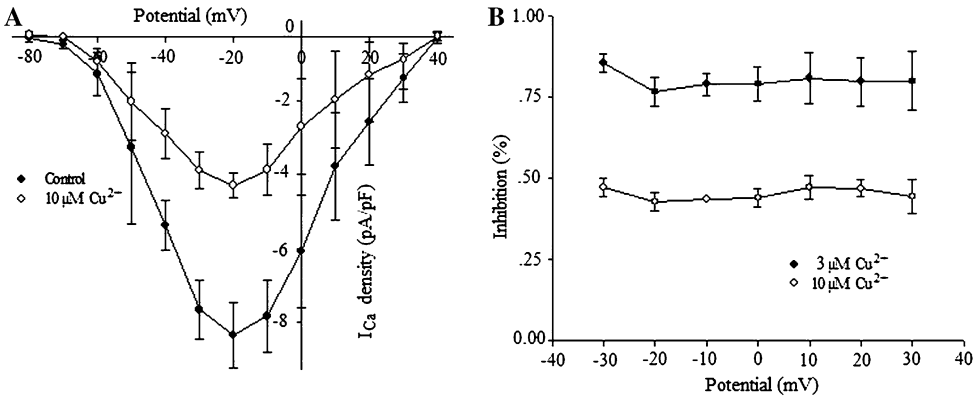

Fig. 3 Effect of Cu^{2+} on $I_{T\text{-}Ca}$ in spermatogenic cells. **a** *I–V* curve for T-type Ca^{2+} currents before and after Cu^{2+} application. Each point represents mean ± SEM from peak Ca^{2+} current normalized by cell capacitance at different test potentials (●, control; ○, 10 μM Cu^{2+}). **b** Peak currents after Cu^{2+} application at each potential were averaged and normalized to control (●, 3 μM Cu^{2+}; ○, 10 μM Cu^{2+})

Activation and Inactivation Kinetics of $I_{T\text{-}Ca}$

T-type Ca^{2+} currents reach a peak after a few milliseconds and decay rapidly, with time courses well fitted by single exponential functions (Fig. 5). With further depolarization, both activation and inactivation rates become faster. To examine the voltage dependence of the kinetic parameters, records were obtained at different potentials and the time constants of activation (τ_m) and inactivation (τ_h) were measured. In control cells, τ_m decreased monotonically with voltage from 57.95 ± 13.50 ms at −50 m*V* to 27.95 ± 1.12 ms at +10 m*V*. Treatment with 10 μM Cu^{2+} decreased τ_m to 50.23 ± 12.75 and 27.73 ± 1.23 ms at −50 and +10 m*V* ($n = 6$, $P < 0.05$), respectively (Fig. 5a). In addition, the time constant of inactivation after 10 μm Cu^{2+} decreased 1.3-fold on average with respect to the control at −40 m*V*. τ_h was 35.18 ± 2.27 and 26.39 ± 1.80 ms for cells before and after 10 μM Cu^{2+} treatment ($n = 5$, $P < 0.05$), respectively (Fig. 5b).

Deactivation Kinetics of $I_{T\text{-}Ca}$

The relaxation of a Ca^{2+} current after removal of membrane depolarization provides information on the gating mechanism of the underlying voltage-gated ion channels. T-type Ca^{2+} channels are distinguished by their relatively slow rate of closing, time constant >1 ms (Chen and Hess 1990; Matteson and Armstrong 1986).

The voltage-dependent kinetics of Ca^{2+} channel closing in spermatogenic cells was measured as the rate of tail current decay at repolarizing potentials. Tail current deactivation could be fitted with single exponentials, whose time constant of decay (τ_d) decreased at more negative repolarization potentials (Fig. 6b). The fact that these tail currents were fitted to single exponential functions at all voltages further supports the notion that the activity of a single class of voltage-gated Ca^{2+} channels underlies the macroscopic Ca^{2+} currents of these cells. The tail current time constant showed strong voltage dependence,

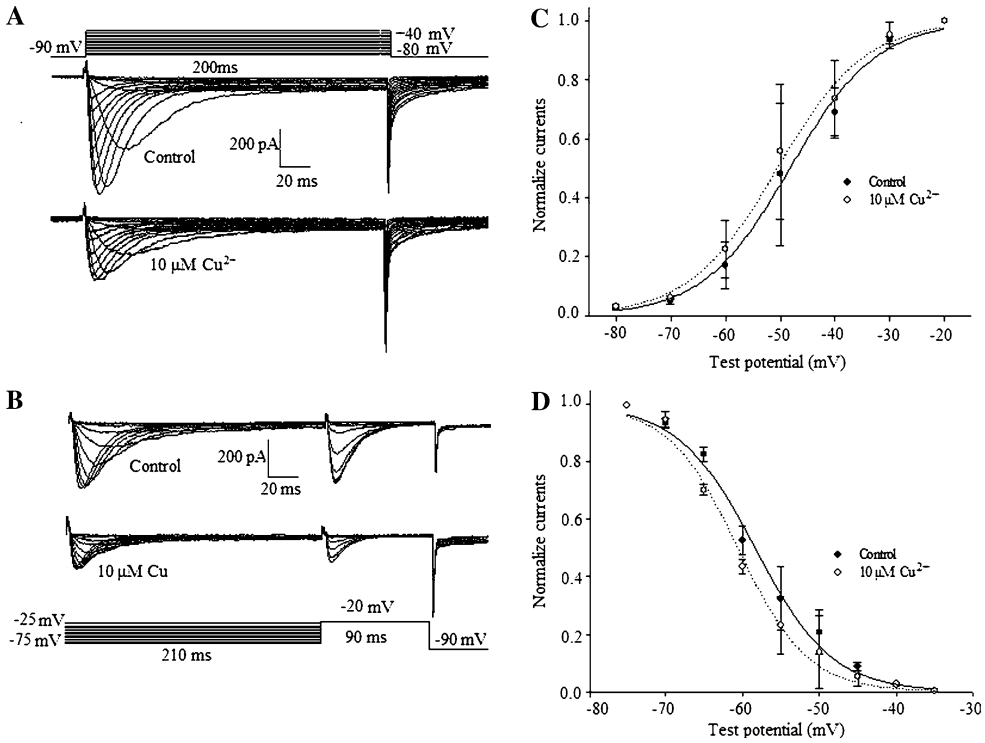

Fig. 4 Voltage-dependent activation and steady-state inactivation of Ca^{2+} currents. **a** Family of current records obtained with activation pulse protocol shown on *top*. These records were used to construct the activation curve. **b** Current records obtained during test pulse to −20 m*V* of inactivation protocol shown on *bottom*. These records were used to construct the steady-state inactivation function. **c** Activation curves. To obtain the activation curve, peak normalized Ca^{2+} conductances were calculated from current records shown in **a** and plotted against command voltage (●, control; ○, 10 μM Cu^{2+}). *Smooth line* was obtained by fitting a Boltzmann relationship to data (see "Materials and Methods"). **d** Inactivation curves. To obtain the steady-state inactivation curve, normalized peak amplitude of currents elicited by the test pulse was plotted as a function of prepulse potential (●, control; ○, 10 μM Cu^{2+}). These data point were fitted with a Boltzmann relationship (see "Materials and Methods")

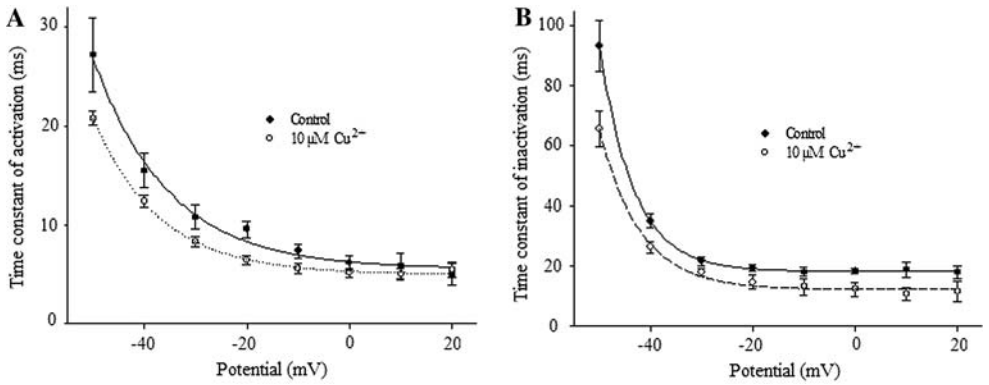

Fig. 5 Voltage dependence of kinetic parameters of activation and inactivation of Ca^{2+} currents. **a** Plot of mean values for the time constant of activation (τ_m) against command voltage. *Smooth line* corresponds to exponential fit of data (●, control; ○, 10 μM Cu^{2+}). **b** Plot of mean values for the time constant of activation (τ_h, obtained by fitting a single exponential to the decay phase of Ca^{2+} currents) vs. step potential (●, control; ○, 10 μM Cu^{2+})

increasing progressively at depolarized potential. The τ_d showed little voltage dependence at potentials less than −85 m*V*. In the experiment shown in Fig. 6a–c, the time constant of channel closing ranged from 4.01 ms at −65 m*V* to 2.12 ms at −100 m*V*. On average, the time constant of deactivation in five spermatogenic cells was 5.53 ± 0.59 ms at −65 m*V* and became shorter at more negative membrane potentials, reaching 2.76 ± 0.28 ms at −100 m*V* (Fig. 6d). Cu^{2+} (10 μM) decreased the time of channel closing at all membrane potentials, ranging from

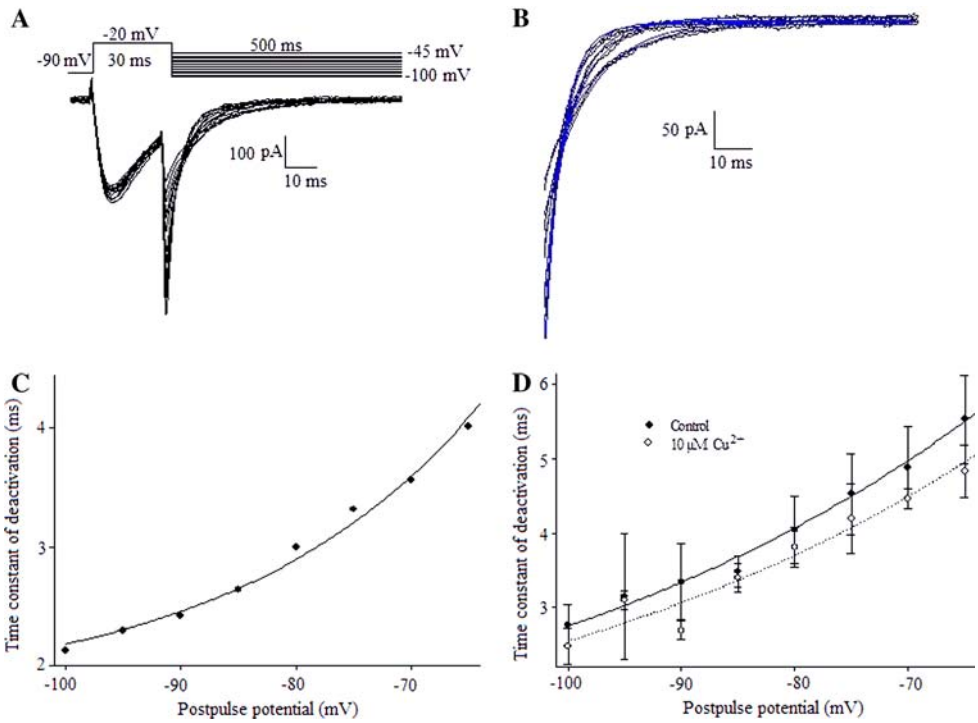

Fig. 6 Voltage dependence of deactivation kinetics. **a** Current records obtained with pulse protocol shown on *top*, designed to measure voltage-dependent kinetics of Ca^{2+} channel closing. Deactivation time constants (τ_d) were determined by fitting a single exponential to tail currents in (**b**). **c** Plot of τ_d vs. repolarization voltage for family of tail currents shown in (**b**). **d** Mean τ_d vs. repolarization potential for six spermatogenic cells (●, control; ○, 10 μM Cu^{2+})

4.83 ± 0.36 ms at −65 m*V* to 2.47 ± 0.24 ms at −100 m*V* ($n = 5$, $P < 0.05$). This result suggests that, as demonstrated in other cell types, deactivation of T-type Ca^{2+} channels present in spermatogenic cells comprises a rapid voltage-independent transition observable only at very negative potentials.

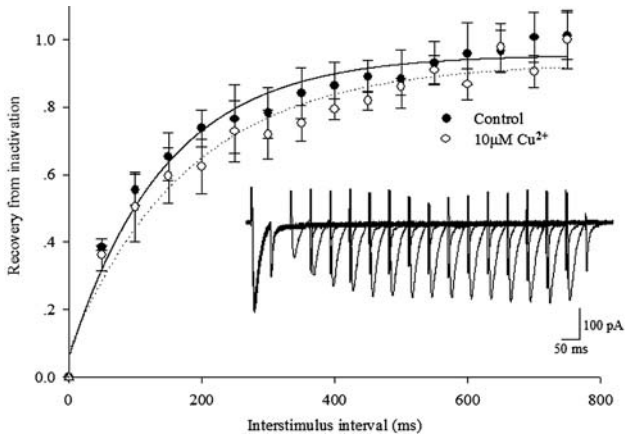

Fig. 7 Recovery from inactivation of Ca^{2+} currents. From a negative holding potential, two voltage pulses to −20 m*V* (conditioning and test pulse) were applied at different interstimulus intervals. *Inset* Superimposed traces from successive trials in an experiment where interstimulus interval was progressively increased. Amplitude of peak current elicited by test pulse, as a fraction of response to conditioning pulse from each trial, is plotted against interval between pulses. These time courses of recovery were fitted by single exponential functions with time constants (τ_r) of 165.68 ± 18.05 (●, control), and 200.85 ± 29.39 (○, 10 μM Cu^{2+}) ms, respectively

Recovery Kinetics of $I_{T\text{-}Ca}$

The recovery from inactivation of Ca^{2+} currents was studied using a double pulse protocol. In Fig. 7, the amplitude of the peak current elicited by the test pulse, as a fraction of the response to the conditioning pulse from each run, is plotted against the length of the interval between pulses. At holding potentials of −110 m*V*, the time courses of recovery can be fitted by single exponential functions with time constants (τ_r) of 165.68 ± 18.05 ms in control. In the presence of 10 μM Cu^{2+}, τ_r increased considerably to 200.85 ± 29.39 ms ($n = 5$, $P < 0.05$).

Discussion

Fertilization involves accurately choreographed cellular interactions required for sperm and egg to fuse and generate a new individual. Gametogenesis occurs in the gonads, where sperm and eggs are produced and where they partially mature. Mammalian sperm undergo further maturation within the female reproductive tract, in a process called "capacitation," to become responsive to the physiological inducer of the AR, the zona pellucida (Yanagimachi 1994; Jungnickel et al. 2003). This maturation process also encompasses parallel changes in the sperm swimming behavior, from an active and symmetric flagellar beat to one more vigorous and asymmetric (Ho and Suarez 2003). After maturation is completed, sperm are ready to contact the egg's extracellular matrix, the zona

pellucida, and undergo the AR, an exocytotic process required in species possessing an acrosome granule, for fertilization to occur (Yanagimachi 1994). T-type Ca^{2+} channels were found to be involved in the male reproduction functions such as the AR, capacitation, motility and fertilization.

As mentioned above, copper plays an important role in male and female reproduction. It has toxic effects on the seminiferous epithelium as well as on the immune system in rams (Telisman et al. 2000). Toxic effects of copper on seminal plasma were manifested in the decrease of motile spermatozoa percentage and in the increase of malformed sperm cells (Jurasovic and Telisman 1993). However, the effects of copper ions on voltage-gated Ca^{2+} channels are much less characterized. In the present study, we found that copper significantly inhibited calcium currents in spermatogenic cells. Here, we report that copper reduces $I_{T\text{-}Ca}$ in mouse spermatogenic cells.

Under the present experimental conditions, Ca^{2+} was the only charge carrier for inward current, which was confirmed by the result that $I_{T\text{-}Ca}$ was not affected by 1 μM Bay K8644 but significantly inhibited by Ni^{2+}-containing solution, together with its low voltage-activated, fast inactivating, steady-state component-free nature (Arnoult et al. 1996; Bai and Shi 2002). Rundown of ionic currents is always a concern in whole-cell voltage-clamp recording. We minimized time-dependent changes in $I_{T\text{-}Ca}$ by using high-resistance pipettes filled with Mg-ATP 4 mM.

In our study, a concentration-dependent blockade of the T-type Ca^{2+} current by Cu^{2+} was demonstrated. The inhibition was mildly voltage-dependent. After 10 μm Cu^{2+} application, the current density of $I_{T\text{-}Ca}$ was significantly reduced by 50%; the steady-state inactivation curve was shifted in the hyperpolarizing direction. In addition, the time constants of activation, inactivation and deactivation were decreased but the time constant of recovery was increased. Thus, copper could inhibit T-type Ca^{2+} current by promoting inactivation and closing and delaying reactivation. To our knowledge, this is the first electrophysiological study directed at the direct effect of Cu^{2+} on Ca^{2+} channel activity in spermatogenic cells.

Our result that copper can directly inhibit T-type Ca^{2+} currents is consistent with a report which shows that copper can directly inhibit the calcium channels in pelvic neurons and HEK 293 cells stably expressing T-type Ca^{2+} channel (Jeong et al. 2003). Recently, Arnoult's group reported that T-type Ca^{2+} current in mouse spermatogenic cells is carried out by the $Ca_V3.2$ subunit (Stamboulian et al. 2004). At the same time, Darszon et al. (2005) reported that the native current in mouse spermatogenic cells may arise from the activity of different types ($Ca_V3.1$, −3.2 and −3.3) of low-threshold channels, with $Ca_V3.2$ contributing around 60%. The present study supports their results. Wennemuth et al. (2000) reported that $Ca_V2.3$ was sensitive to Ni^{2+} and expressed in mouse spermatogenic cells. Also, it was likely sensitive to Cu^{2+}. $Ca_V2.3$ belongs to the HVA family. At present, there is no electrophysiological proof supporting that the expression of $Ca_V2.3$ with some subunits can produce currents resembling the T-type Ca^{2+} current. Thus, we can rule out the contribution of $Ca_V2.3$. As we know, T-type Ca^{2+} channels play a key role in the reproductive function; our results suggest that Cu^{2+}-induced blockade of Ca^{2+} channels might lead to a toxic effect on sperm and, hence, to antifertility capacity.

In conclusion, this is the first report to electrophysiologically detail the inhibitory effects of copper on T-type Ca^{2+} channels in mouse spermatogenic cells. Taken together, our results provide ionic evidence of a possible link between the reproductive effect of copper and T-type calcium channels. It is reasonable that copper might be a potential agent influencing reproduction such as the AR and the capacitation of sperm through T-type Ca^{2+} channels as a contraceptive drug.

Acknowledgements This work was supported by the National Science Foundation of China (30571555 and 30771831).

References

Arnoult C, Cadullo RA, Lemos JR, Florman HM (1996) Activation of mouse sperm T-type Ca^{2+} channels by adhesion to the egg zona pellucida. Proc Natl Acad Sci USA 93:13004–13009

Arnoult C, Villaz M, Florman HM (1998) Pharmacological properties of the T-type Ca^{2+} current of mouse spermatogenic cells. Mol Pharmacol 53:1104–1111

Bai JP, Shi YL (2002) Inhibition of T-type Ca^{2+} currents in mouse spermatogenic cells by gossypol, an antifertility compound. Eur J Pharmacol 440:1–6

Chen C, Hess P (1990) Mechanism of gating of T-type calcium channels. J Gen Physiol 96:603–630

Darszon A, Nishigaki T, Wood C, Trevino CL, Felix R, Beltran C (2005) Calcium channels and Ca^{2+} fluctuations in sperm physiology. Int Rev Cytol 243:79–172

Darszon A, Lopez-Martinez P, Acevedo JJ, Hernandez-Cruz A, Trevino CL (2006) T-type Ca^{2+} channels in sperm function. Cell Calcium 40:241–252

Ebesh O, Barone A, Harper RG, Wapnir R (1999) Combined effect of high-fat diet and copper deficiency during gestation on fetal copper status in the rat. Biol Trace Elem Res 67:139–150

Espinosa F, Lopez-Gonzalez I, Serrano CJ, Gasque G, De La Vega-Beltran JL, Trevino CL, Darszon A (1999) Anion channel blockers differentially affect T-type Ca^{2+} currents of mouse spermatogenic cells, a1E currents expressed in *Xenopus* oocytes and the sperm acrosome reaction. Dev Genet 25:103–114

Espinosa F, Lopez-Gonzalez I, Munoz-Garay C, Felix R, De La Vega-Beltran JL, Kopf GS, Visconti PE, Darszon A (2000) Dual regulation of the T-type Ca^{2+} current by serum albumin and hestradiol in mammalian spermatogenic cells. FEBS Lett 475:251–256

Hart EB (1928) Copper as a supplement to iron for hemoglobin building in the rat. J Biol Chem 77:797–812

Ho HC, Suarez SS (2003) Characterization of the intracellular calcium store at the base of the sperm flagellum that regulates hyperactivated motility. Biol Reprod 68:1590–1596

Hostetler CE, Kincaid RL, Mirando MA (2003) The role of essential trace elements in embryonic and fetal development in livestock. Vet J 166:125–139

Jeong SW, Park BG, Park JY, Lee JW, Lee JH (2003) Divalent metals differentially block cloned T-type calcium channels. Neuroreport 14:1537–1540

Jungnickel MK, Sutton KA, Florman HM (2003) In the beginning: lessons from fertilization in mice and worms. Cell 114:401–404

Jurasovic J, Telisman S (1993) Determination of lead and cadmium in human seminal fluid by electrothermical atomic absorption spectrometry. J Anal At Spectrom 8:419–425

Lievano A, Santi CM, Serrano CJ, Trevino CL, Bellve AR, Hernandez-Cruz A, Darszon A (1996) T-type Ca^{2+} channels and a1E expression in spermatogenic cells, and their possible relevance to the sperm acrosome reaction. FEBS Lett 388:150–154

Matteson DR, Armstrong CM (1986) Properties of two types of calcium channels in clonal pituitary cells. J Gen Physiol 87:161–182

Roblero L, Guadarrama A, Lopez T, Zegers-Hochschild F (1996) Effect of copper ion on the motility, viability, acrosome reaction and fertilizing capacity of human spermatozoa in vitro. Reprod Fertil Dev 8:871–874

Santi CM, Darszon A, Hernandez-Cruz A (1996) A dihydropyridine-sensitive T-type Ca^{2+} current is the main Ca^{2+} current in mouse primary spermatocytes. Am J Physiol 271:1583–1593

Stamboulian S, Kim D, Shin HS, Ronjat M, De Waard M, Arnoult C (2004) Biophysical and pharmacological characterization of spermatogenic T-type calcium current in mice lacking the $Ca_V3.1$ (alpha1G) calcium channel: $Ca_V3.2$ (alpha1H) is the main functional calcium channel in wild-type spermatogenic cells. J Cell Physiol 200:116–124

Telisman S, Cvitkovic P, Jurasovic J, Pizent A, Gavella M, Rocic B (2000) Semen quality and reproductive endocrine function in relation to biomarkers of lead, cadmium, zinc, and copper in men. Environ Health Perspect 108:45–53

Thomas JW, Moss S (1951) The effect of orally administered molybdenum on growth spermatogenesis and testes histology of young dairy bulls. J Dairy Sci 34:929–934

Wennemuth G, Wenstenbroek RE, Xu T, Hille B, Babcock DF (2000) $Ca_V2.2$ and $Ca_V2.3$ (N- and R-type) Ca^{2+} channels in depolarization-evoked entry of Ca^{2+} into mouse sperm. J Biol Chem 275:21210–21217

Wong WY, Flik G, Groenen PM, Swinkels DW, Thomas CM, Copius-Peereboom JH, Merkus HM, Steeqers-Theunissen RP (2001) The impact of calcium, magnesium, zinc and copper in blood and seminal plasma on semen parameters in men. Reprod Toxicol 15:131–136

Yanagimachi R (1994) Mammalian fertilization. In: Knobile E, Neill JD (eds) The physiology of reproduction. Raven Press, New York, pp 189–317